BRL MR 2345

BRL

MEMORANDUM REPORT NO. 2345

THE HUGONIOT OF 5083 ALUMINUM

by

George Hauver
Angelo Melani

December 1973

USA BALLISTIC RESEARCH LABORATORIES
ABERDEEN PROVING GROUND, MARYLAND

Destroy this report when it is no longer needed.
Do not return it to the originator.

Secondary distribution of this report by originating or sponsoring activity is prohibited.

Additional copies of this report may be obtained from the National Technical Information Service, U.S. Department of Commerce, Springfield, Virginia 22151.

The findings in this report are not to be construed as an official Department of the Army position, unless so designated by other authorized documents.

The use of trade names or manufacturers' names in this report does not constitute indorsement of any commercial product.

BALLISTIC RESEARCH LABORATORIES

MEMORANDUM REPORT NO. 2345

DECEMBER 1973

THE HUGONIOT OF 5083 ALUMINUM

George Hauver
Angelo Melani

Terminal Ballistics Laboratory

RDT&E Project No. 1W062113A659

ABERDEEN PROVING GROUND, MARYLAND

BALLISTIC RESEARCH LABORATORIES

MEMORANDUM REPORT NO. 2345

GHauver & AMelani/bst
Aberdeen Proving Ground, Md.
December 1973

THE HUGONIOT OF 5083 ALUMINUM

ABSTRACT

The Hugoniot of 5083H131 aluminum has been experimentally determined in the pressure range from 161 to 472 kilobars. Over this pressure range the shock velocity-particle velocity relationship was found to be linear. The optical and electrical techniques used for the measurements and the methods for data reduction are described. A revised Hugoniot for polymethylmethacrylate and an approximate Hugoniot for mica were required in the electrical technique and are included as appendixes.

TABLE OF CONTENTS

		Page
	ABSTRACT	3
	LIST OF ILLUSTRATIONS	7
	LIST OF TABLES	9
	LIST OF SYMBOLS	11
I.	INTRODUCTION	13
II.	PROCEDURE	13
	A. Test Material	13
	B. Shock Systems	15
	C. Optical Measurements	15
	D. Electrical Measurements	19
III.	RECORD REDUCTION AND ANALYSIS	23
	A. Optical Measurements	23
	B. Electrical Measurements	25
	C. Impedance Calculations	28
IV.	RESULTS AND CONCLUSIONS	29
	APPENDIX A. Revised Hugoniot for Polymethylmethacrylate	33
	APPENDIX B. Hugoniot for Mica	35
	REFERENCES	37
	DISTRIBUTION LIST	39

LIST OF ILLUSTRATIONS

Figure		Page
1.	Experimental Arrangement for Optical Measurements, Schematically Showing the Shock Velocity Specimen and the Offset Strip of Buffer Metal Used to Detect Free-Surface Displacement.	16
2.	Streak-Camera Record from the Hugoniot Test on 5083 Aluminum Performed at 472 Kilobars.	17
3.	Experimental Arrangement for Electrical Measurements of Shock Velocity in Specimens of PMMA and 5083 Aluminum	20
4.	Signals from PMMA and Mica Recorded in Electrical Measurements of Shock Velocity. A - PMMA at 63 Kilobars (161 Kilobars in 5083 Al); B - Mica (5083 Al at 161 Kilobars); C - Mica (5083 Al at 227 Kilobars).	22
5.	A Single, Idealized, Nonplanar Image on a Streak-Camera Record, Indicating the Required Measurements.	24
6.	Geometry of the Situation in which an Unconfined Shock-Velocity Specimen is Obliquely Impacted by a Plane Shock Wave	26
7.	The Hugoniot Data for 5083 Aluminum Plotted in the Shock Velocity-Particle Velocity Plane.	30
8.	Comparison of the Hugoniots for 5083 Aluminum, 2024 Aluminum, and Mica in the Pressure-Particle Velocity Plane	31
B-1.	Shock-Induced Electrical Signals from Mica Recorded in Hugoniot Tests at 193 kilobars (A) and 463 Kilobars (B).	36

LIST OF TABLES

		Page
I.	Chemical Composition of 5083 Specimens	14
II.	Hugoniot Data for 5083 Aluminum	29
A-I.	Hugoniot Data for Plexiglas II UVA	34
B-I.	Hugoniot Data for Mica	35

LIST OF SYMBOLS

d	displacement on film record, mm
t	time, μsec
u	particle velocity, mm/μsec
u_f	free-surface velocity, mm/μsec
C	sound speed, mm/μsec
D	free-surface displacement, mm
L	radial distance from lateral boundary, mm
P	pressure, kbar
S	camera writing speed, mm/μsec
T	time interval, μsec
U	shock wave velocity, mm/μsec
W	diameter, mm
X	thickness, mm
α	angle between shock front and interface, degree
γ	Gruneisen coefficient
θ	angle between sweep direction and normal to image surface, degree
ρ	density, g/cc

Subscript "$_o$" refers to the initial condition.

I. INTRODUCTION

Measurements have been performed to determine the Hugoniot of 5083H131 aluminum over a pressure range from 161 to 472 kilobars. This pressure range is above the elastic-plastic double wave region which extends from the Hugoniot Elastic Limit to approximately 127 kilobars. The 5083 aluminum alloy nominally contains 4.5 percent magnesium and 0.7 percent manganese; the H131 designates a special temper which has been used for armor (this temper designation will not be used in later references to the test material). This report describes the experimental procedures, explains the reduction of data, and presents the results.

II. PROCEDURE

Hugoniot data were obtained by the impedance-matching technique[1*]. In each test, a specimen of 5083 aluminum was placed on a metal plate, referred to as a buffer, through which a plane shock wave was transmitted. Either optical or electrical measurements were performed to locate the release adiabat of the buffer and to determine the average velocity of the shock wave transmitted through the test specimen. The average shock velocity, U, and the initial density, ρ_o, establish a line with slope $\rho_o U$ in the P-u (pressure-particle velocity) plane. An impedance calculation establishes the intersection of this line with the release adiabat of the buffer. This intersection is a point on the Hugoniot curve of the test specimen.

A. Test Material

Test specimens of 5083 aluminum were prepared from a plate with the chemical composition** given in Table I. This composition is within the tolerances set by the Aluminum Association specification. The initial density of 5083 aluminum specimens was measured to be 2.656 g/cc.

---

*References are listed on page 37

**Analyzed by the Materials Laboratory, U. S. Army Frankford Arsenal.

Table I. Chemical Composition of 5083 Aluminum Specimens

Element	Percent Content
Magnesium	4.12
Manganese	0.65
Iron	0.2/0.4
Silicon	0.05/0.15
Zinc	<0.1
Copper	<0.1
Titanium	<0.1
Chromium	0.05/0.15
Nickel	<0.02
Lead	<0.02
Tin	none detected
Aluminum	remainder

B. Shock Systems

The highest test pressure (472 kbar) was produced by plate impact. In this test, a 20-cm diameter plane wave lens with a 5-cm thick booster of plastic-bonded HMX was used to accelerate a 4.9-mm thick "flying plate" of 2024 aluminum. After 3-cm of travel, this "flying plate" impacted a 5.3-mm thick buffer plate of 2024 aluminum which held the test specimens. Lower shock pressures were produced by detonating an explosive charge in contact with a 6.35-mm thick buffer plate holding the test specimen. In contact-detonation experiments, the explosive consisted of a 10-cm diameter plane wave lens with a 2.54-cm thick booster of either 75/25 Octol or TNT. The buffer plates were either 2024 aluminum or free-cutting brass (ASTM Number B16).

C. Optical Measurements

An optical technique[5] was used in several experiments to determine the average shock velocity through test specimens and the free-surface velocity of the buffer plate. The experimental arrangement for optical measurements is indicated in Figure 1. This technique utilized changes in surface reflectivity to detect shock arrival. Free surfaces of the buffer and mounted specimens were lapped to produce diffuse reflectivity, illuminated by an explosive-argon light source, and observed with a rotating-mirror streak camera writing at 10mm/μsec.

Shock velocity specimens were 3.2mm thick and 12.7mm in diameter with faces plane and parallel within 2.5 microns. These specimens were attached to the surface of the buffer plate by a fillet of epoxy (Hysol Epoxi-Patch 608) with care so that the epoxy did not extend into the line of observation. After attaching the specimen, the distance from the specimen surface to the buffer was measured and compared with the specimen thickness to verify that no dust or epoxy had been introduced at the interface. Figure 2 is the streak camera record from the test performed at 472 kilobars. The images produced by the shock velocity specimens are identified as A, C, and E.in this figure.

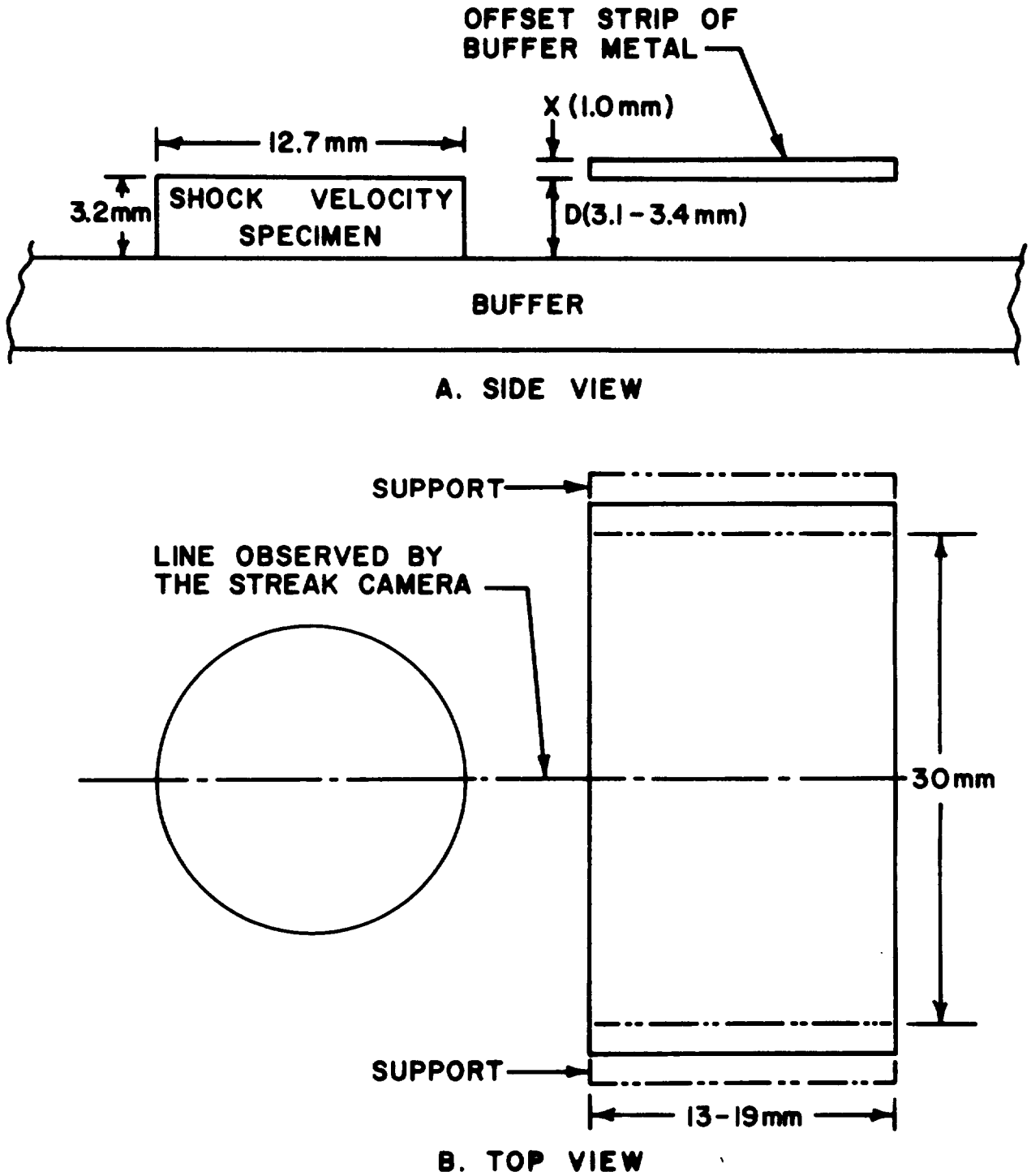

Figure 1. Experimental Arrangement for Optical Measurements, Schematically Showing the Shock Velocity Specimen and the Offset Strip of Buffer Metal Used to Detect Free-Surface Displacement

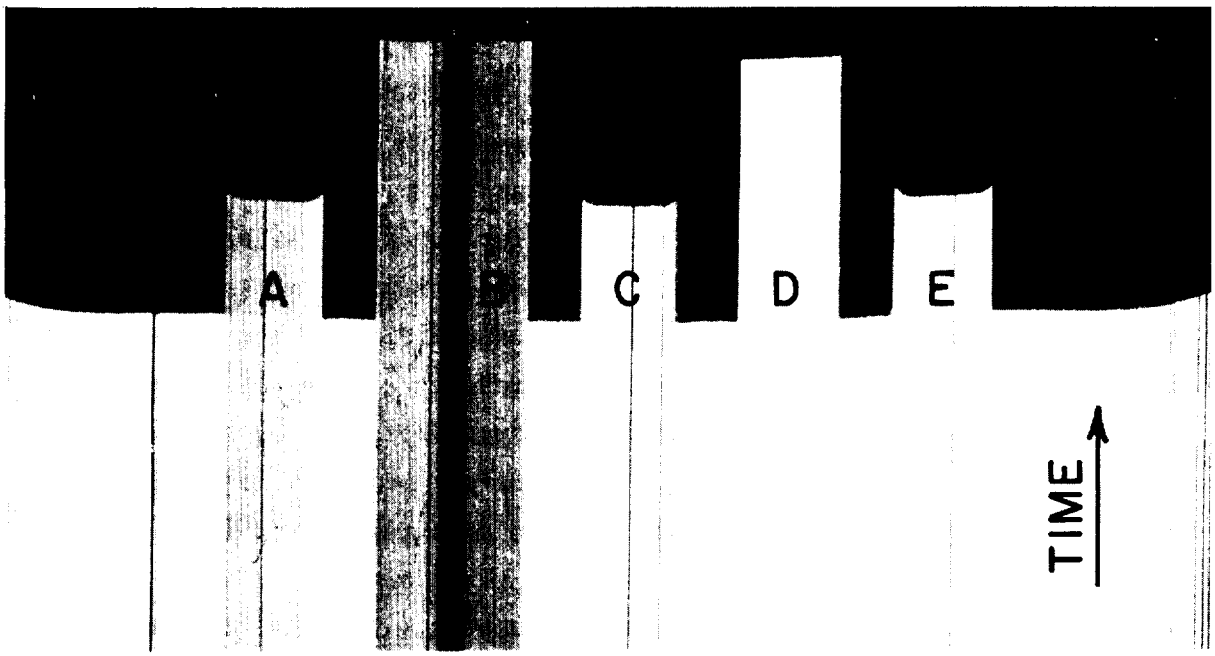

A,C,E — SHOCK VELOCITY MEASUREMENTS

B,D — FREE-SURFACE VELOCITY MEASUREMENTS

Figure 2. Streak-Camera Record from the Hugoniot Test on 5083 Aluminum Performed at 472 Kilobars

If free surface velocity of the buffer plate was to be measured, a thin strip of the buffer metal was supported above the buffer surface. This experimental arrangement is shown in Figure 1. As indicated in the figure, the offset distance, D, was 3.1 to 3.4mm; the thickness, X, was 1.0mm; and the width of the offset strip was 13 to 19mm. The exposed surface of the strip was lapped, prior to assembly, to match the finish and presumably the reflectivity of the buffer surface. After assembly, the distance (D + X) was verified by measurements with an electrically-indicating depth micrometer. Changes in reflectivity at the free surfaces of the buffer and offset strip provided a measure of the total time interval, T, required for free-surface excursion through distance, D, and for shock travel through thickness, X. Free-surface velocity measurements are identified in Figure 2 as B and D. The obscured region in the center of B in Figure 2 is caused by a bar which braced the strip to insure flatness between the points of support. However, the braced and unbraced strips yielded the same free-surface velocity within 0.2 percent.

Uniform image density on streak camera records was not always achieved. Areas of different image density are evident in the streak record shown in Figure 2. When measurements are performed between image areas of unequal density, an error caused by halation is possible. However, the close agreement of the two free-surface velocities and the narrow spread of the three shock velocities in the test at 472 kilobars suggested that any halation-related error was minimal.

The reflectivity change utilized by this technique is well defined only at higher pressures. At 472 kilobars in 5083 aluminum, the shock-induced reflectivity change was sharply defined (See Figure 2). At 285 kilobars in brass (167 kbar in 5083 aluminum), the reflectivity change upon shock arrival at the 5083 aluminum surface was still well defined, but definition at the brass surface was only marginal.

An advantage of this technique is the nearly continuous observation of shock arrival along the buffer surface and across the offset strips and shock velocity specimens. The only troublesome area occurs near

the lateral boundary of the shock velocity specimens where lateral pressure release delays shock arrival at the free surface. However, the influence of this inherent boundary effect is minimized by the technique, and it is believed that the nearly continuous observation of shock arrival reduces the measurement error associated with nonplanarity of the shock front.

D. Electrical Measurements

An electrical technique was first introduced at the lower pressures where optical definition became marginal, and was used later in tests at higher pressures. This technique utilized shock-induced electrical signals[2,3,4] to measure the average shock velocity through test specimens. The shock velocity through specimens of 5083 aluminum was used to establish the $\rho_o U$ line in the P-u plane. A material with a known Hugoniot was placed beside the 5083 aluminum on the buffer; the shock velocity through this test material established its Hugoniot state and located the release adiabat of the buffer.

Polymethylmethacrylate (PMMA) was used as the reference material. The PMMA selected was Rohm and Haas type II UVA Plexiglas in sheet form. This particular brand had been selected for prior study.[5] Subsequent tests indicated that the commercially available stock of this particular PMMA was suitably reproducible, and since then it has served as a reference material. The density of the PMMA was measured to be 1.183 g/cc. Its Hugoniot, in the pressure range of the current tests, is given by the linear relationship $U = 2.695 + 1.538u$ (See Appendix A), in which the velocity unit is mm/μsec.

The experimental arrangement for electrical measurements is shown in Figure 3. PMMA test specimens were 3.2mm thick and 12.7mm in diameter with faces flat and parallel within 2.5 microns. The specimen was used as the dielectric of a parallel plate capacitor. The buffer plate served as one electrode; the other electrode was an air-dried coating of silver paint (Silpaint 2065-01, Sel Rex Corp., Electronic Materials Division) on the specimen. Electrical connection to the painted electrode

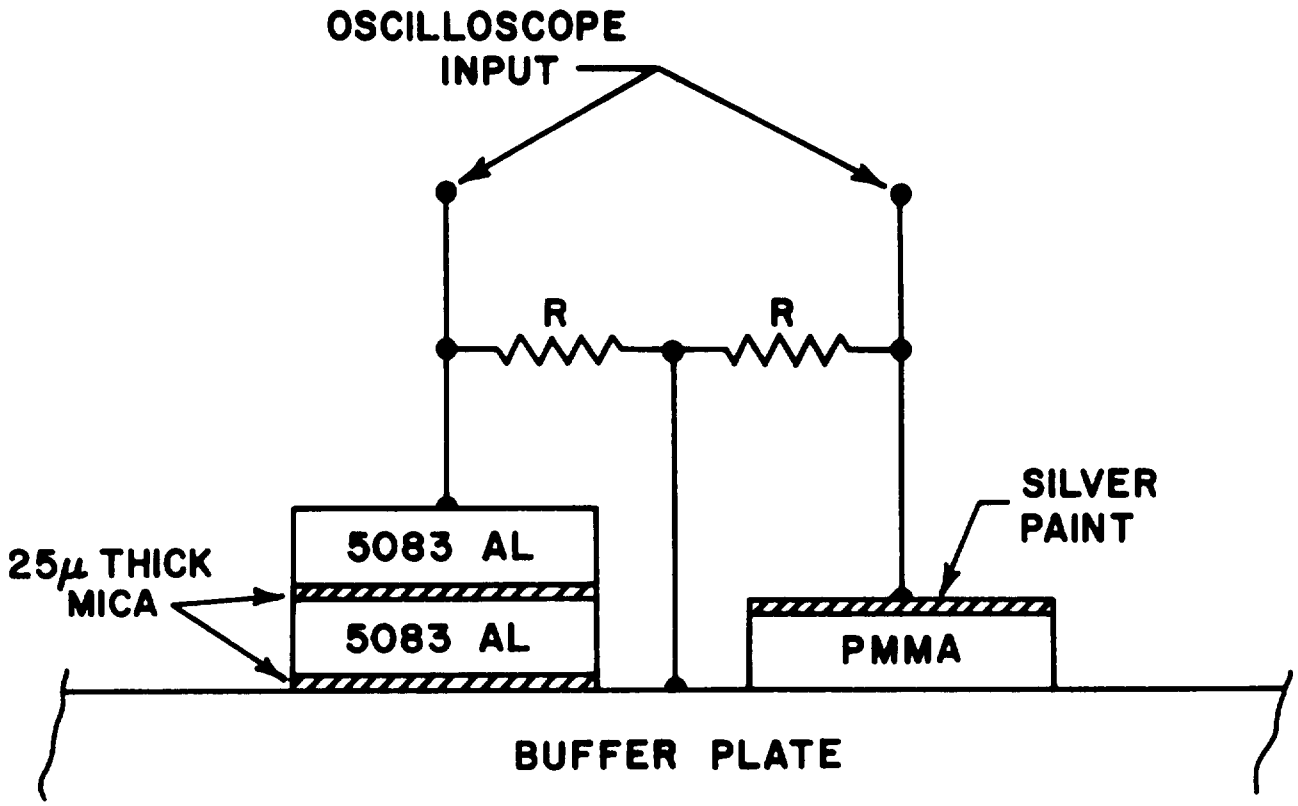

Figure 3. Experimental Arrangement for Electrical Measurements of Shock Velocity in Specimens of PMMA and 5083 Aluminum

was made by a spring contact, and the two electrodes were connected through a load resistor, R (the terminating resistor of the RG-213/U signal cable; R = 50 ohms). A shock-induced electrical signal from PMMA is shown in Figure 4-A. The signal begins at t_1 when the shock front enters the PMMA from the buffer and abruptly changes amplitude at t_3 when the shock front arrives at the painted electrode. The recording oscilloscope had a bandwidth of 150 MHz, cable lengths did not exceed six meters, and the circuit risetime was less than one nanosecond. Consequently, the risetime of the recorded PMMA signal could usually be related to the nonplanarity of the incident shock front (Here, and in later references to nonplanarity, the buffer surface serves as the reference plane). Knowing the specimen dimensions, the signal risetime and duration could be used to calculate the transit time, and subsequently the shock velocity.

The 5083 aluminum specimens prepared for the electrical measurements had the same dimensions as those prepared for the optical measurements. As shown in Figure 3, a 2.5-micron thick mica sheet was placed on either side of a 5083 aluminum specimen. Arrival of the shock front at each mica sheet produced an electrical signal which was recorded by an oscilloscope. Mica was selected as the dielectric because it is conveniently available in thin sheets and has a shock impedance which, in the pressure range of these tests, is only 15 percent higher than the shock impedance of 5083 aluminum. The approximate Hugoniot of this mica was established by two measurements which are reported in Appendix B. The transit time of the shock wave through the mica sheet was interpreted to be less than the time difference for shock arrival across the specimen diameter. The short transit time, the long risetime of the mica circuit, and the erratic amplitude variations of the mica signal, prevented the signal risetime from being reliably related to the nonplanarity of the incident shock front. Therefore, the risetime of the signal from the nearby PMMA specimen provided an estimate of nonplanarity over the area of the 5083 aluminum specimen. Fortunately, the calculated shock velocity is reasonably insensitive to errors in the

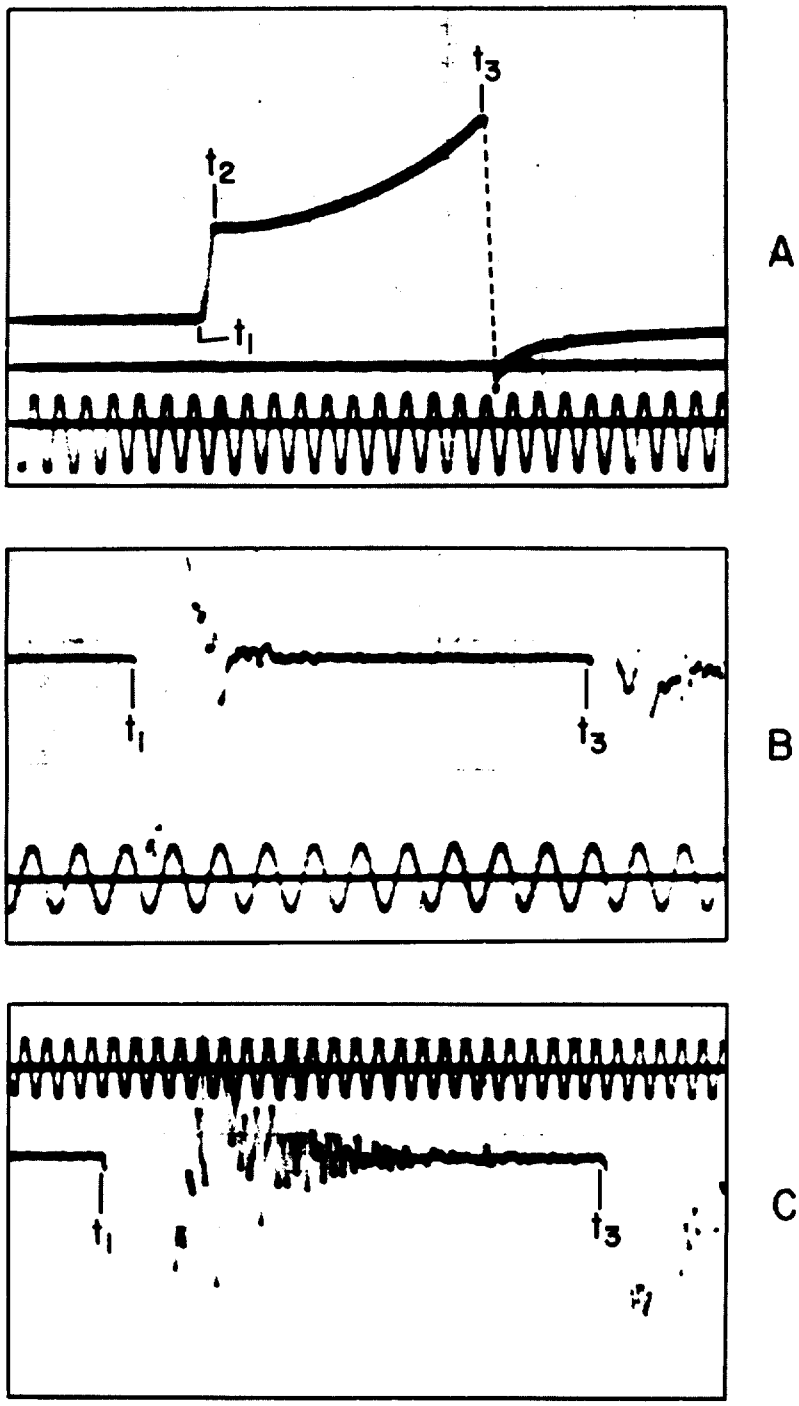

Figure 4. Signals from PMMA and Mica Recorded in Electrical Measurements of Shock Velocity. A--PMMA at 63 Kilobars (161 Kilobars in 5083 Al); B--Mica (5083 Al at 161 Kilobars); C--Mica (5083 Al at 227 Kilobars)

nonplanarity correction used to determine the transit time. Figure 4, B and C, show oscilloscope records of mica signals from tests at 161 and 227 kilobars. Times t_1 and t_3 on the records indicate the arrival times of the shock front at each of the two mica sheets.

III. RECORD REDUCTION AND ANALYSIS

A. Optical Measurements

Streak camera records were measured on a McPherson optical comparator. With care, it was found that measurements could be reproduced to approximately ±13 microns. Referring to Figure 2, it is seen that the shock front is not perfectly plane, but is characterized by a slight waviness or nonplanarity. A single, idealized, nonplanar image is shown in Figure 5. The comparator crosshair is aligned first along the cut-off line produced by shock arrival at the buffer free surface, and then shifted to the cut-off line produced by shock arrival at the specimen surface, giving the film displacement d_1. The normal to these image surfaces is displaced from the sweep direction by an angle θ_1. The measurement is repeated at the other side of the specimen image, giving d_2 and θ_2. The transit time, T, is given by

$$T = \left[(d_1/\cos\theta_1) + (d_2/\cos\theta_2)\right] / 2S,$$

where S is the camera writing speed.

In determining the shock velocity, it was always assumed that the path length was negligibly different from the specimen thickness. This assumption is justified by the nonplanarity observed by the streak camera. Unfortunately, the streak camera does not detect nonplanarity about an axis parallel to the line of observation. However, electrical measurements can detect the total nonplanarity and, across a 12.7-mm diameter specimen, 50 nanoseconds is seldom exceeded. It is assumed that nonplanarity can usually be treated as obliquity over short distances on the buffer surface. Under normal conditions, this nonplanarity indicates a shock obliquity of less than two degress in the specimen. Within this

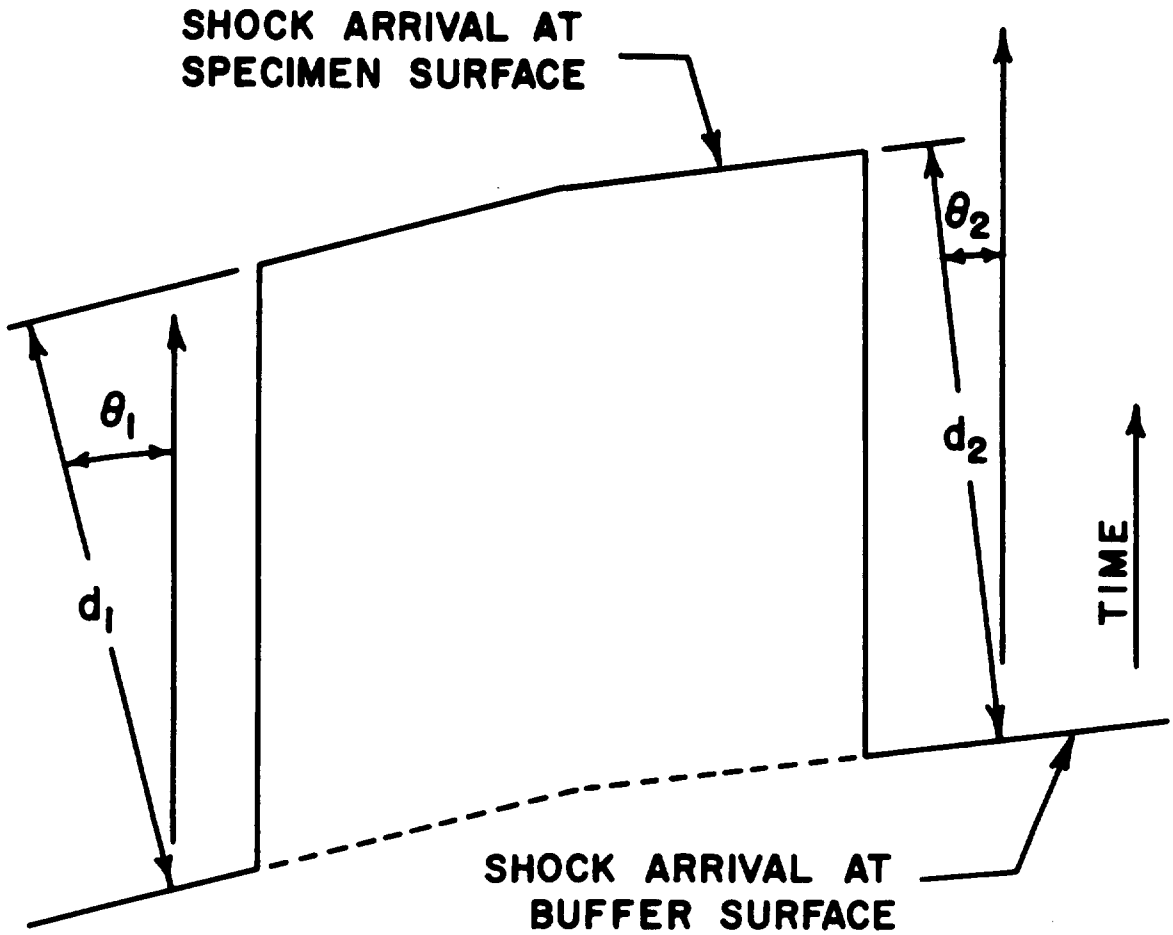

Figure 5. A Single, Idealized, Nonplanar Image on a Streak-Camera Record, Indicating the Required Measurements

angle of obliquity, the shock path differs from the specimen thickness by less than 0.1 percent which is negligible.

In free-surface velocity measurements, the measured time interval, T, was the total time for free-surface excursion across the offset distance, D, and for shock wave travel through the strip thickness, X. The free-surface velocity u_f was obtained from the expression,

$$u_f = D \Big/ \left[T - (X/U) \right],$$

where U is the shock velocity through the offset strip of buffer metal. This shock velocity was initially estimated; values for both U and u_f were then improved by iteration.

B. Electrical Measurements

Several shock-induced electrical signals from the tests are shown in Figure 4. Figure 4-A is the signal from a PMMA reference specimen. The signal begins at time t_1 when the shock front first arrives at the buffer-specimen interface. Because of nonplanarity, the shock front does not enter the specimen simultaneously over the entire interface area. Instead, it enters the specimen over a time interval $(t_2 - t_1)$ which is usually the risetime of the PMMA signal. Only infrequently does the measured risetime equal the risetime of the 150 MHz oscilloscope which displays the signal. The shock front arrives at the second electrode (painted electrode) of the specimen at time t_3. The transit time of the shock wave through the PMMA specimen can be obtained from times t_1, t_2, and t_3. In the case of electrical signals from mica (Figure 4, B and C), only times t_1 and t_3 are determined. In the analysis of these signals, $(t_2 - t_1)$ was inferred from the electrical signal of the PMMA which was located close to the 5083 aluminum specimen.

Figure 6 illustrates the situation in which an unconfined specimen is obliquely impacted by a plane shock wave from the buffer. The shock front arrives at the buffer-specimen interface first at point M, and the electrical signal begins at this time, t_1. At time t_2, the shock front has

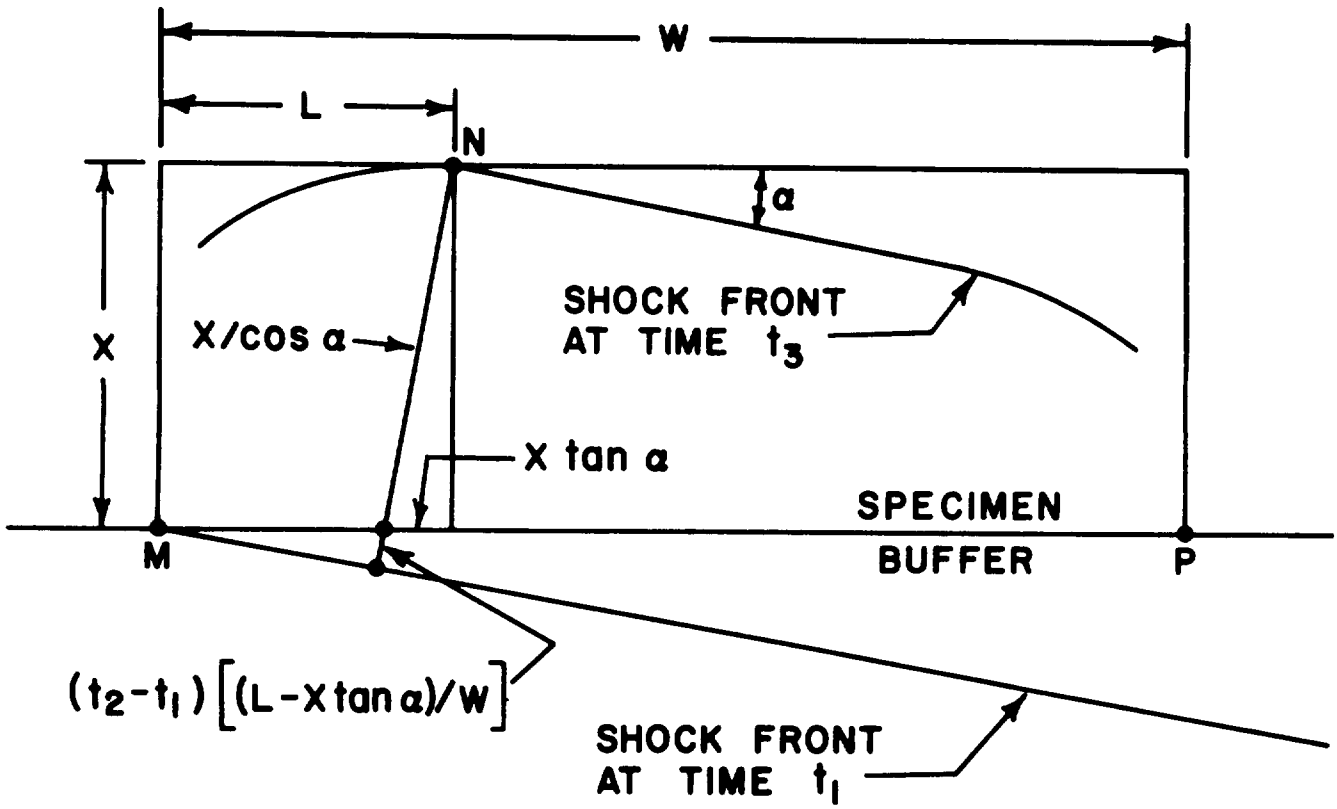

Figure 6. Geometry of the Situation in which an Unconfined Shock Velocity Specimen is Obliquely Impacted by a Plane Shock Wave

reached point P and the shock wave has entered the specimen over the full interface area. In the specimen, the angle between the shock front and the interface is α. A rarefaction originates at the unconfined lateral boundary, relieves the compression, reduces the shock wave velocity, and causes the shock front to curve back in a region near the lateral boundary. Because of this curvature, the shock front arrives at the rear surface of the specimen first at point N which is a radial distance L in from the lateral boundary. The arrival time at point N is t_3. Time interval $(t_3 - t_1)$, the full duration of the shock-induced electrical signal, exceeds the shock transit time, T. From Figure 6, it is seen that T is given by,

$$T = (t_3 - t_1) - (t_2 - t_1) \quad (L - X \tan \alpha)/W,$$

where W is the specimen diameter. If the angle α is small (about one degree), $X \tan \alpha << L$, since $X \simeq L$, and $X/\cos \alpha \simeq X$. Therefore,

$$U \simeq X \; / \; [(t_3 - t_1) - (t_2 - t_1)\; L/W].$$

With little error, L can be determined from the special case where $\alpha = 0$. The lateral rarefaction, which begins first at point M, travels at the local sound velocity, C, to reach N. The distance $MN = C(t_3 - t_1) = CX/U$. The path MN is effectively the hypotenuse of the triangle with one side equal to L and the other side equal to the shock-compressed thickness $X(\rho_o/\rho)$, where ρ_o is the initial density and ρ is the density under shock compression. Then,

$$CX/U = [L^2 + X^2 \; (\rho_o/\rho)^2]^{1/2} \quad .$$

Rearranging,

$$L = X \; [(C/U)^2 - (\rho_o/\rho)^2]^{1/2} \quad .$$

In reducing the data, it was initially assumed that $U = X/(t_3 - t_1)$. Then, C and (ρ_o/ρ) were evaluated by assuming an approximate Hugoniot for 5083 aluminum. It was actually assumed that the Hugoniot for 5083

aluminum could be approximated by the Hugoniot for 2024 aluminum. This approximation introduced errors in L of 1.9 percent at 161 kilobars, 1.1 percent at 300 kilobars, and 0.6 percent at 472 kilobars. These errors are insignificant because the shock velocity is insensitive to small errors in L. For the measurements on 5083 aluminum, it was found that a 100 percent error in the obliquity correction [$L\ (t_2 - t_1)/W$] introduced an error in U which did not exceed 1.3 percent. It was this insensitivity to the obliquity correction which justified the use of $(t_2 - t_1)$ from the PMMA signals to calculate the obliquity correction for transit time measurements on specimens of 5083 aluminum.

C. Impedance Calculations

The Hugoniot points for 5083 aluminum were obtained by impedance calculations. In each test the shock velocity in 5083 aluminum was measured and used to establish the line with a slope $\rho_o U$ in the P-u plane. This line intersected the release adiabat of the buffer at the Hugoniot state in 5083 aluminum. The release adiabat of the buffer was located either at $(P-P_o) = 0$ by a free-surface velocity measurement, or at $(P-P_o) > 0$ by establishing the Hugoniot state in a PMMA reference specimen included on the buffer. Release adiabats were generated by assuming a constant $\gamma\rho$, where γ is the Gruneisen coefficient and ρ is density. Data used for the two buffer metals were:

2024 Aluminum:	$\rho_o = 2.785$ g/cc	$\gamma_o = 1.89$
	$U = 5.328 + 1.338u$	(Reference 6)
Brass:	$\rho_o = 8.443$ g/cc	$\gamma_o = 1.84$
	$U = 3.802 + 1.418u$	

However, brass was used only at the lowest test pressure which was 273 kilobars (in the brass). At this pressure, the release curve was found to be represented adequately by the Hugoniot.

IV. RESULTS AND CONCLUSIONS

The Hugoniot data for 5083 aluminum are listed in Table II, and plotted in the U-u plane in Figure 7. The data are also plotted in

TABLE II

Hugoniot Data for 5083 Aluminum

Shock Velocity mm/μsec	Particle Velocity mm/μsec	Pressure kilobar
6.527	0.961	167
6.553	0.926	161
7.027	1.218	227
7.448	1.528	302
7.489	1.556	310
8.206	2.158	470
8.244	2.154	472
8.248	2.154	472
8.250	2.153	472

the P-u plane in Figure 8 for comparison with the Hugoniots of 2024 aluminum and mica. The data in the U-u plane are interpreted to define a straight line which is represented by the relationship,

$$U = 5.297 + 1.372\ u,$$

where the velocity unit is mm/μsec and the standard deviation of U, σ_U, is 0.054. A casual inspection of Figure 7 suggests that a quadratic expression might provide a better fit to the data points. However, it is doubtful that a quadratic fit is justified. The standard deviation of 0.054 obtained with a linear fit is consistent with the values of σ_U usually obtained in mixed measurements of this type. Mixed optical and electrical measurements have been found to yield a σ_U in the range from 0.049 to 0.058[7,8]. When only electrical measurements were performed, σ_U was found to lie in the range from 0.049 to 0.062[9]; when only optical measurements were performed, values

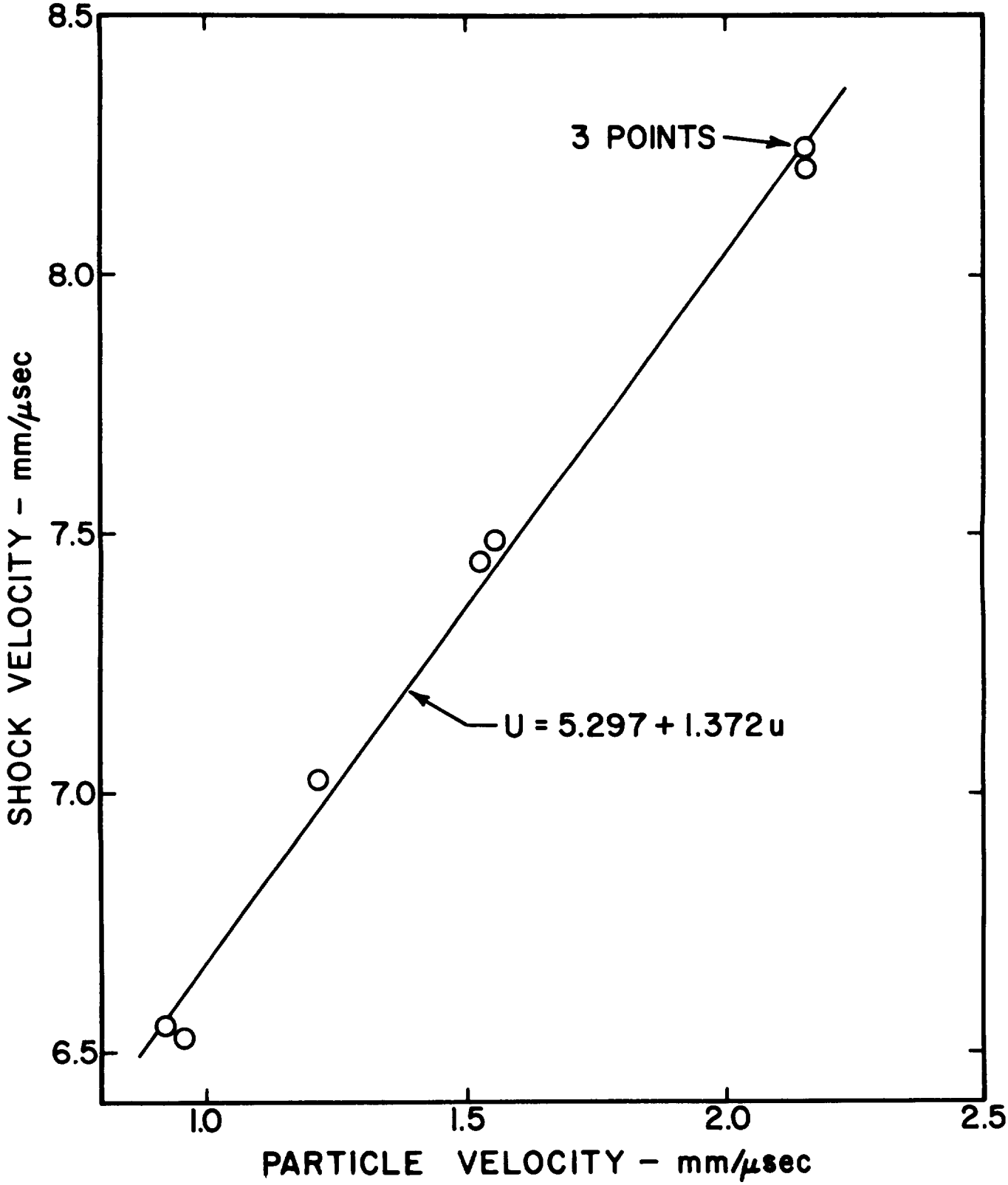

Figure 7. The Hugoniot Data for 5083 Aluminum Plotted in the Shock Velocity-Particle Velocity Plane

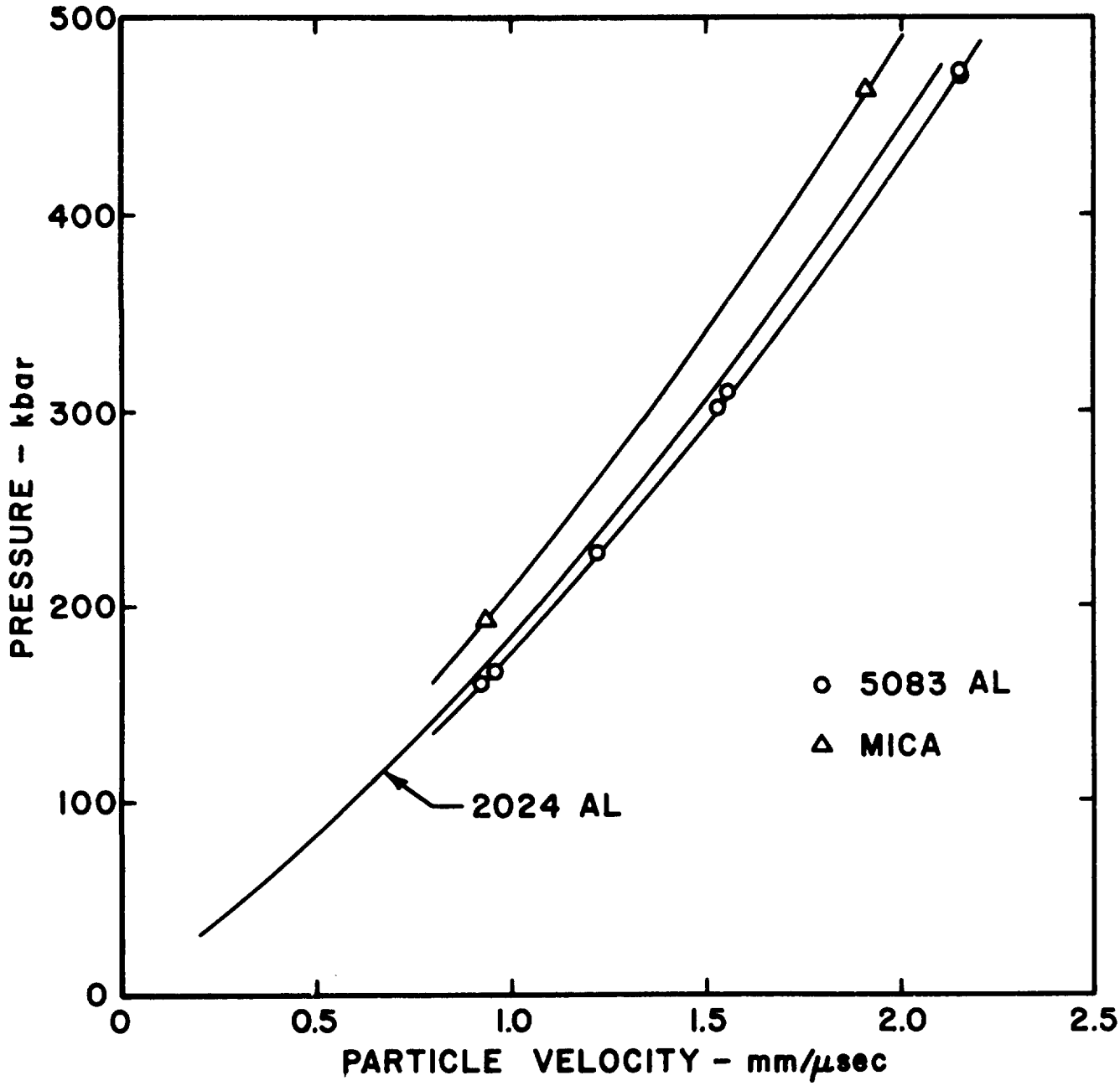

Figure 8. Comparison of the Hugoniots for 5083 Aluminum, 2024 Aluminum, and Mica in the Pressure-Particle Velocity Plane

of 0.042 and 0.044 were obtained[8]. The higher limit on the range for electrical measurements is believed to relate to uncertainty about the nature of nonplanarity. While nonplanarity has been treated as oblique incidence, it can also result from various degrees of curvature which cannot be taken into account. The pressure-volume states defined by the Hugoniot of 5083 aluminum may be expressed in the alternate form,

$$P = 747.3\mu + 1239.2\mu^2 + 1212.0\mu^3 ,$$

where $\mu = (\rho/\rho_o) - 1$, and P is the pressure in kilobars.

APPENDIX A

Revised Hugoniot for PMMA

A shock Hugoniot for PMMA (Plexiglas II UVA) was reported by the authors in 1964[5]. Since that time, new equation-of-state data for the buffer metals have been reported. Consequently, the Hugoniot data for Plexiglas II UVA have been reexamined and revised. For the impedance calculations, release adiabats for the buffer metals were generated using the following data:

AZ31B Magnesium:	ρ_o = 1.776 g/cc	γ_o = 1.64
	U = 4.648 + 1.198u	
2024 Aluminum:	ρ_o = 2.785 g/cc	γ_o = 1.89
	U = 5.328 + 1.338u	(Reference 6)
Free-cutting Brass:	ρ_o = 8.443 g/cc	γ_o = 1.84
	U = 3.802 + 1.418u	
Copper:	ρ_o = 8.93 g/cc	γ_o = 1.96
	U = 3.940 + 1.489u	(Reference 6)

The revised Hugoniot data and the relative weight assigned to each data point are listed in Table A - I. These data lie below the phase transition in the pressure range from 43 to 185 kilobars. Within this pressure range the Hugoniot of Plexiglas II UVA is represented by the linear relationship,

$$U = 2.695 + 1.538u,$$

where the velocity unit is mm/μsec.

TABLE A - I

Hugoniot Data for Plexiglas II UVA

Shock Velocity mm/ sec	Particle Velocity mm/ sec	Weight
4.047	0.890	1
4.500	1.135	1
4.514	1.160	1
4.930	1.468	1
4.503	1.766	1
5.407	1.838	1
5.469	1.814	2
5.653	1.966	2
5.692	1.884	2
5.794	2.035	2
6.016	2.174	2
6.088	2.201	1
6.319	2.320	1
6.423	2.437	2
6.484	2.378	1

APPENDIX B

Hugoniot for Mica

Two tests were performed to approximately locate the shock Hugoniot of mica (Muscovite, Tanzania Green, Quality V_2, ρ_o = 2.86 g/cc). These tests were performed electrically using the experimental arrangement for PMMA measurements shown in Figure 2. Mica specimens, 1.0mm thick and 5.1mm in diameter, were machined from block mica taking care not to delaminate the crystal planes. The shock velocity through a PMMA (Plexiglas II UVA) specimen was measured to locate the buffer cross curve in each test. These PMMA reference specimens were 1.0mm thick and 7.0mm in diameter.

The shock tests with mica were performed at 193 and 463 kilobars (in mica). Shock-induced electrical signals from the mica specimens are shcwn in Figure B-1. Figure B-1A is the signal recorded at 193 kilobars. This signal provides clear evidence of both positive and negative components[10,11]. The initial break at time t_1 is in the negative direction, while the break at time t_3 is in the positive direction. Time t_2 is indicated, but is doubtful in this test. Figure B-1B is the signal recorded at 463 kilobars. This signal also gives evidence of both positive and negative components. Times t_1, t_2, and t_3 are indicated in the figure. It is suspected that the amplitude fluctuations between t_1 and t_3 may have resulted from variations in impurity content through the crystal thickness. The Hugoniot data are listed in Table B - I and plotted in Figure 8 for comparison with the Hugoniots of 5083 and 2024 aluminums. The full curve plotted in Figure 8 was obtained by assuming a linear U-u relationship based on the two data points and is intended only to approximate the actual Hugoniot.

TABLE B - I

Hugoniot Data for Mica

Shock Velocity mm/μsec	Particle Velocity mm/μsec	Pressure kilobar
7.210	0.936	193
8.465	1.911	463

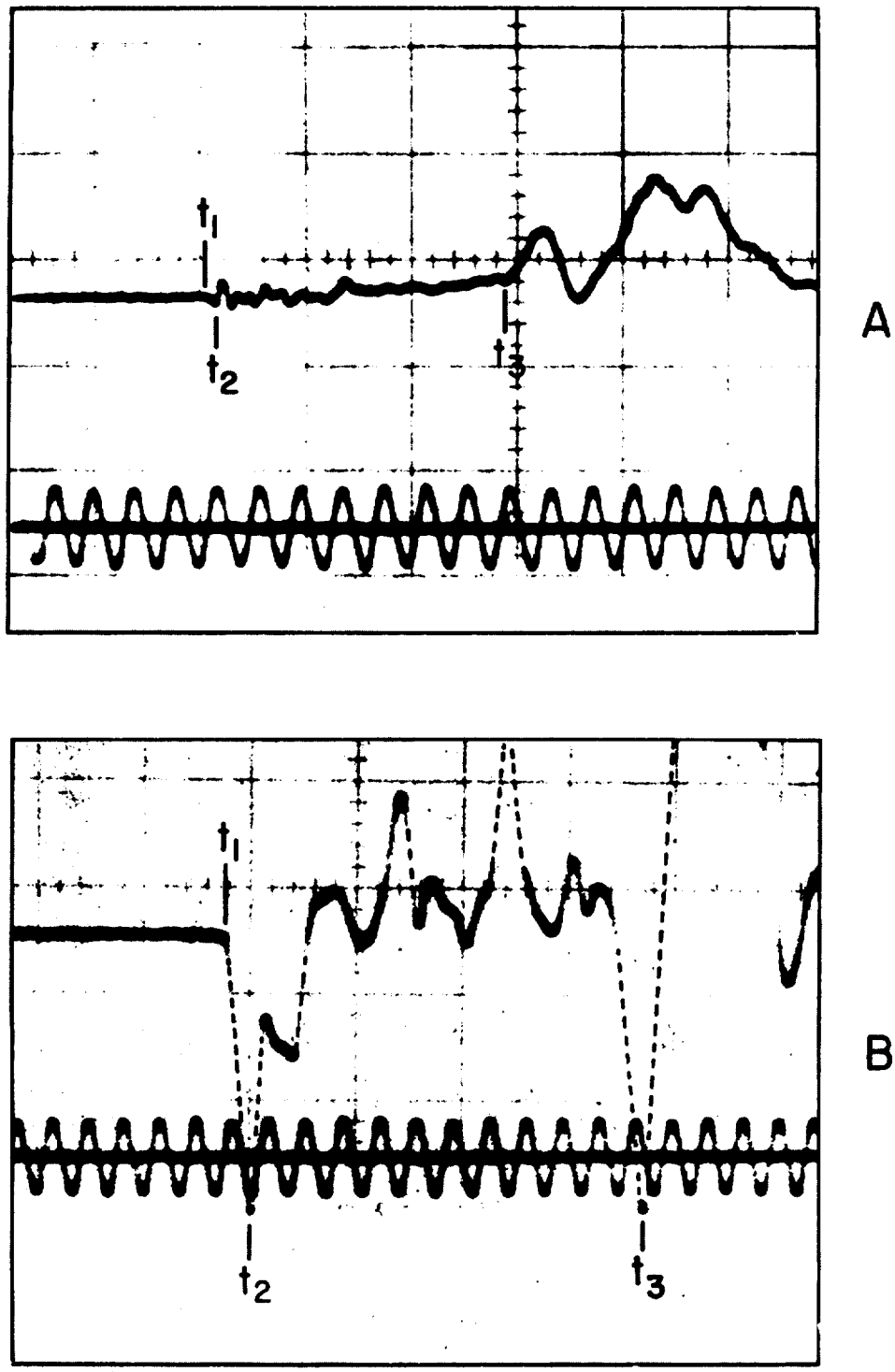

Figure B-1. Shock-Induced Electrical Signals from Mica Recorded in Hugoniot Tests at 193 kilobars (A) and 463 Kilobars (B)

REFERENCES

1. J. M. Walsh, M. H. Rice, R. G. McQueen, and F. L. Yarger, "Shock-Wave Compression of Twenty-Seven Metals. Equations of State of Metals", Phys. Rev., Vol. 108, 1957, 196 - 216.

2. G. E. Hauver, "Characteristics of Several Dielectric Materials at High Pressure", Ballistic Research Laboratories Technical Note No. 1356, October 1960. (AD #248025)

3. R. J. Eichelberger and G. E. Hauver, "Solid State Transducers for Recording of Intense Pressure Pulses", Les Ondes de Detonation, 15 Quai Anatole-France, Paris, Editions Du Centre National De La Recherche Scientifique, 1962, 363 - 382.

4. G. E. Hauver, "Shock-Induced Polarization in Plastics. II. Experimental Study of Plexiglas and Polystyrene", J. Appl. Phys., Vol. 36, 1965, 2113 - 2118.

5. G. E. Hauver and A. Melani, "Shock Compression of Plexiglas and Polystyrene", Ballistic Research Laboratories Report No. 1259, August 1964. (AD #609194)

6. W. J. Carter, S. P. Marsh, J. N. Fritz, and R. G. McQueen, "The Equation of State of Selected Materials for High-Pressure References", Accurate Characterization of the High-Pressure Environment, Proceedings of a Symposium held at the National Bureau of Standards, Gaithersburg, Maryland, October 14-18, 1968, National Bureau of Standards Special Publication 326, Issued March 1971, 147 - 158.

7. G. E. Hauver and A. Melani, "The Shock Hugoniot of Single-Crystal Lithuim Fluoride", Ballistic Research Laboratories Memorandum Report No. 2058, August 1970. (AD #712320)

8. G. E. Hauver and A. Melani, "The Shock Hugoniot of Single-Crystal Sodium Chloride", Ballistic Research Laboratories Memorandum Report No. 2061, August 1970. (AD #713599)

9. G. E. Hauver and A. Melani, Unpublished Hugoniot data for several polyethylenes.

10. G. E. Hauver, "Shock-Induced Polarization Signals with Positive and Negative Components", Ballistic Research Laboratories Memorandum Report No. 2074, November 1970. (AD #716329)

11. G. E. Hauver, "Shock-Induced Electrical Signals from Dielectrics", Preprints - The Fifth Detonation Symposium, August 18-21, 1970, Pasadena, California, ONR Report DR-163. 313 - 322.

DISTRIBUTION LIST

No. of Copies	Organization
12	Commander Defense Documentation Center ATTN: DDC-TCA Cameron Station Alexandria, Virginia 22314
2	Director of Defense Research and Engineering (OSD) ATTN: Dir, Tech Information Strategic and Space Systems Division Washington, DC 20301
2	Director Defense Nuclear Agency ATTN: Mr. J. Moulton Mr. J. Kelso Washington, DC 20301
1	Commander U.S. Army Materiel Command ATTN: AMCDL 5001 Eisenhower Avenue Alexandria, Virginia 22304
1	Commander U.S. Army Materiel Command ATTN: AMCRD, MG S. C. Meyer 5001 Eisenhower Avenue Alexandria, Virginia 22304
1	Commander U.S. Army Materiel Command ATTN: AMCRD, Dr.J.V.R.Kaufman 5001 Eisenhower Avenue Alexandria, Virginia 22304
1	Commander U.S. Army Materiel Command ATTN: AMCRD-T 5001 Eisenhower Avenue Alexandria, Virginia 22304
1	Commander U.S. Army Materiel Command ATTN: AMCRD-WN-RE-1 Mr. G. Burke 5001 Eisenhower Avenue Alexandria, Virginia 22304
1	Commander U.S. Army Materiel Command ATTN: AMCRD-WN-RE, J. Corrigan 5001 Eisenhower Avenue Alexandria, Virginia 22304
1	Commander U.S. Army Aviation Systems Command ATTN: AMSAV-E 12th and Spruce Streets St. Louis, Missouri 63166
1	Director U.S. Army Air Mobility Research and Development Laboratory Ames Research Center Moffett Field, California 94035
1	Commander U.S. Army Electronics Command ATTN: AMSEL-RD Fort Monmouth, New Jersey 07703
3	Commander U.S. Army Missile Command ATTN: AMSMI-R AMSMI-RSS, Mr. Cobb AMCPM-PE Redstone Arsenal, Alabama 35809
2	Commander U.S. Army Tank Automotive Command ATTN: AMSTA-RHFL; AMSTA-CL Warren, Michigan 48090

DISTRIBUTION LIST

No. of Copies	Organization
1	Commander U.S. Army Mobility Equipment Command ATTN: AMSME-R 4300 Goodfellow Boulevard St. Louis, Missouri 63120
2	Commander U.S. Army Mobility Equipment Research & Development Center ATTN: Tech Docu Cen, Bldg. 315 AMSME-RZT Fort Belvoir, Virginia 22060
1	Commander U.S. Army Armament Command Rock Island, Illinois 61202
1	Commander U.S. Army Frankford Arsenal ATTN: Dr. R. Donnard Philadelphia, Pennsylvania 19137
1	Commander U.S. Army Picatinny Arsenal ATTN: SARPA-VA6 Dover, New Jersey 07801
1	Commander U.S. Army Sentinel Systems Command ATTN: SENSC, J. Davidson P. O. Box 1500 Huntsville, Alabama 35807
1	Commander U.S. Army Safeguard Systems Command ATTN: LTC W. Alfonte Redstone Arsenal, Alabama 35809
1	Commander Safeguard Systems Office Washington, DC 20000
1	Director U.S. Army Advanced Materiel Concepts Agency 5001 Eisenhower Avenue Alexandria, Virginia 22314
1	Commander U.S. Army Harry Diamond Laboratories ATTN: AMXDO-TI Washington, DC 20438
2	Commander U.S. Army Materials and Mechanics Research Center ATTN: AMXMR-ATL AMXMR-ED, J. Dignam Watertown, Massachusetts 02172
1	Commander U.S. Army Natick Laboratories ATTN: AMXRE, Dr. D. Sieling Natick, Massachusetts 01762
1	Director U.S. Army Advanced Ballistic Missile Defense Agency ATTN: CRDABH-5, Mr. Loomis P. O. Box 1500 Huntsville, Alabama 35809
2	HQDA (DARD-MD COL M. Kortum Dr. S. Alexander) Washington, DC 20310
2	HQDA (DARD-ARP-P; Dr. T. Sullivan) Washington, DC 20310

DISTRIBUTION LIST

No. of Copies	Organization
1	Commander U.S. Army Research Office (Durham) Box CM, Duke Station Durham, North Carolina 27706
1	HQDA (DARD-MS Nike-X & Space Division) Washington, DC 20310
3	Commander U.S. Naval Air Systems Command ATTN: AIR-604 Washington, DC 20360
3	Commander U.S. Naval Ordnance Systems Command ATTN: ORD-9132 Washington, DC 20360
2	Commander U.S. Naval Ship Research and Development Center ATTN: Code 823, Dr. Myles M. Marwitz Code 735, Dr. J. Thomas Washington, DC 20007
1	Commander U.S. Naval Ship Research and Development Center ATTN: Mr. L. T. Butt Underwater Expl Rsch Div Portsmouth, Virginia 23709
1	Commander U.S. Naval Ordnance Laboratory ATTN: Mr. J. W. Forbes Silver Spring, Maryland 20910
1	Director U.S. Naval Research Laboratory ATTN: Wave Propagation Br Mr. Macdonald Washington, DC 20390
1	Commander U.S. Navy Marine Engineering Laboratory ATTN: Dr. Yung-Fa Wang Code 832.4 Annapolis, Maryland 21402
1	Commander, NAVSEC ATTN: Dr. Chiu, Code 6129 Prince George's Center Hyattsville, Maryland 20782
1	HQ USAF (AFNIE-CA) Washington, DC 20330
3	AFWL (WLA; WLD; CTP S. Washington) Kirtland AFB New Mexico 87117
1	SAMSO (CPT W. Crichlow) Norton AFB California 92409
1	SAMSO (SMT-STINFO) Los Angeles AFB California 90045
1	ASD (ASBES) Wright-Patterson AFB Ohio 45433
1	AFFDL (Dr. R. Bader) Wright-Patterson AFB Ohio 45433

DISTRIBUTION LIST

No. of Copies	Organization
1	Headquarters U.S. Atomic Energy Commission Washington, DC 20545
1	Director Lawrence Radiation Laboratory P. O. Box 808 Livermore, California 94550
1	Director Los Alamos Scientific Lab P. O. Box 1663 Los Alamos, New Mexico 87544
1	Director NASA Scientific and Technical Information Facility ATTN: SAK/DL P. O. Box 33 College Park, Maryland 20740
1	Director NASA Langley Research Center ATTN: Dr. M. Stein Langley Station Hampton, Virginia 23365
1	J. G. Engineering Research Associates 3831 Menlo Drive Baltimore, Maryland 21215
2	Sandia Laboratories ATTN: Info Distr Div Code 5510, Mr. Peurifoy P. O. Box 5800 Albuquerque, New Mexico 87115
1	Systems, Science & Software ATTN: Dr. J. K. Dienes P. O. Box 1620 La Jolla, California 92307
1	Brown University Division of Engineering ATTN: Prof. P. Symonds Providence, Rhode Island 02912
1	Franklin Institute Research Laboratories ATTN: Dr. Zenon Zudans The Benjamin Franklin Pkwy Philadelphia, Pennsylvania 19103
1	North Carolina State Univ School of Engineering ATTN: Dr. T. Sun Chang Raleigh, North Carolina 27607
1	Southwest Research Institute ATTN: Dr. W. Baker 8500 Culebra Road San Antonio, Texas 78206
1	Stanford Research Institute Poulter Laboratory 333 Ravenswood Avenue Menlo Park, California 94205
1	University of Delaware Department of Mechanical Engineering ATTN: Prof. J. Vinson Newark, Delaware 19711
1	University of Florida ATTN: Prof. L. Malvern Gainesville, Florida 32601
1	University of Notre Dame Dept of Metallurgical Engineering & Materials Sciences ATTN: Dr. N. F. Fiore Notre Dame, Indiana 46556

DISTRIBUTION LIST

Aberdeen Proving Ground
Ch, Tech Lib
Marine Corps Ln Ofc
Dir, USAMSAA

Unclassified

Security Classification

DOCUMENT CONTROL DATA - R & D

(Security classification of title, body of abstract and indexing annotation must be entered when the overall report is classified)

1. ORIGINATING ACTIVITY *(Corporate author)* Ballistic Research Laboratories Aberdeen Proving Ground, MD 21005	2a. REPORT SECURITY CLASSIFICATION Unclassified 2b. GROUP

3. REPORT TITLE

"The Hugoniot of 5083 Aluminum"

4. DESCRIPTIVE NOTES *(Type of report and inclusive dates)*

Memorandum Report

5. AUTHOR(S) *(First name, middle initial, last name)*

George E. Hauver and Angelo Melani

6. REPORT DATE	7a. TOTAL NO. OF PAGES	7b. NO. OF REFS
DECEMBER 1973	43	11

8a. CONTRACT OR GRANT NO. b. PROJECT NO. 1W062113A659 c. d.	9a. ORIGINATOR'S REPORT NUMBER(S) Memorandum Report No. 2345 9b. OTHER REPORT NO(S) *(Any other numbers that may be assigned this report)*

10. DISTRIBUTION STATEMENT

Approved for public release; distribution unlimited.

11. SUPPLEMENTARY NOTES	12. SPONSORING MILITARY ACTIVITY
	U.S. Army Materiel Command 5001 Eisenhower Avenue Alexandria, Virginia 22304

13. ABSTRACT

The Hugoniot of 5083H131 aluminum has been experimentally determined in the pressure range from 161 to 472 kilobars. Over this pressure range the shock velocity-particle velocity relationship was found to be linear. The optical and electrical techniques used for the measurements and the methods for data reduction are described. A revised Hugoniot for polymethylmethacrylate and an approximate Hugoniot for mica were required in the electrical technique and are included as appendixes.

DD FORM 1 NOV 68 1473 REPLACES DD FORM 1473, 1 JAN 64, WHICH IS OBSOLETE FOR ARMY USE.

Unclassified

Security Classification

14. KEY WORDS	LINK A		LINK B		LINK C	
	ROLE	WT	ROLE	WT	ROLE	WT
5083 Aluminum						
Hugoniot						
Shock-induced electrical signals						
Mica Hugoniot						
Polymethylmethacrylate Hugoniot						
Streak Camera Measurements						